Proceedings of the
International Conference on Mechanical Engineering 2011
(ICME2011) 18-20 December 2011, Dhaka, Bangladesh

ICME11-TH-021

MHD HEAT AND MASS TRANSFER UNSTEADY FLOW OF A MICROPOLAR FLUID THROUGH A POROUS MEDIUM WITH INDUCED MAGNETIC FIELD

Md. Mohidul Haque and Md. Mahmud Alam

Mathematics Discipline, Khulna University, Khulna, Bangladesh

ABSTRACT

MHD free convective heat and mass transfer unsteady flow of a micropolar fluid past an infinite vertical porous plate through a porous medium has been observed under the action of a strong magnetic field taking into account the induced magnetic field with a constant heat source. It is considered that the porous plate is subjected to constant heat and mass fluxes. The mathematical model of the problem is solved numerically by the unconditionally stable implicit finite difference method. The approximate value of all the flow variables as velocity, angular velocity, induced magnetic field, fluid temperature and species concentration are computed in this work. Also the profiles of the above mentioned quantities are shown in figures and the effects of important parameters on the flow variables are discussed briefly. Finally, a comparison with previous work is tabulated here.

Keywords: MHD Heat and Mass Transfer, Micropolar Fluid, Porous Medium, Induced Magnetic Field

1. INTRODUCTION

The induced magnetic field is arisen due to a strong magnetic field. The study with induced magnetic field is of great interest in astrophysics and geophysics to investigate the stellar and solar structures, interstellar matter, radio propagation through the ionosphere etc. Since the problems with induced magnetic field play a decisive role in a number of industrial applications such as fiber or granular insulation, liquid-metals, electrolytes, ionized gases as well as the geothermal systems, Chaudhary and Sharma[1] have studied the induced magnetic field effect on a combined heat and mass transfer steady flow over a vertical plate with constant heat and mass fluxes. Numerical solutions of the same problem in case of two dimensional flows have been calculated by Alam et al.[2]. Recently, the induced magnetic field effects on mixed convective transient heat and mass transfer flow with constant heat and mass fluxes have been investigated by Haque and Alam[3].

Micropolar fluids are those, which contain dilute suspension of small, rigid, cylindrical macromolecules with individual motions that support stress and body moments, which are influenced by spin inertia. Eringen[4] was the first author to propose a theory of molecular fluids taking into account the inertial characteristics of the substructure particles, which are allowed to undergo rotation. Physically, the micropolar fluids contain suspended metal or dust particles. It has many practical applications, for example analyzing the behavior of exotic lubricants, the flow of colloidal suspensions or polymeric fluids, liquid crystals, additive suspensions, human or animal blood and turbulent shear flow. The free convective micropolar fluid flow induced by the simultaneous action of buoyancy forces is of great interest in nature and in many industrial applications as drying processes, solidification of binary alloy as well as in astrophysics, geophysics and oceanography. Jena and Mathur[5] obtained a similarity solution for laminar free convective flow of thermo-micropolar fluid from a non-isothermal vertical flat plate. A free convective mass transfer flow for a micropolar fluid bounded by a vertical surface under the action of a transverse magnetic field is observed by El-Amin[6]. Quit recently, an unsteady free convective heat and mass transfer flow of a micropolar fluid through a porous medium under the action of a transverse magnetic field with a constant heat source has been investigated by Haque et al.[7]. In the present work we want to apply a strong magnetic field that induced another magnetic field on the above problem.

Hence our aim is to investigate the thermal diffusion effect on the free convective heat and mass transfer MHD unsteady flow of a micropolar fluid past an infinite vertical porous plate through a porous medium in the present of a strong magnetic field with constant heat and mass fluxes.

2. MATHEMATICAL MODEL

A transient free convective heat and mass transfer MHD flow of electrically conducting, incompressible, viscous micropolar fluid past an electrically non-

conducting infinite vertical porous plate bounded by a porous medium with a constant heat source is considered here. The flow is assumed to be in the *x*-direction, which is chosen along the plate in upward direction and *y*-axis is normal to it. A strong uniform magnetic field is applied normal to the flow region that induced another magnetic field **H** . Initially, it is considered that the fluid particles and the plate are at rest at same temperature $\overline{T} = T_\infty$ with same concentration level $\overline{C} = C_\infty$ at all points, where T_∞ and C_∞ are fluid temperature and species concentration of uniform flow respectively. The physical configuration and coordinate system of the problem is presented in Fig. 1.

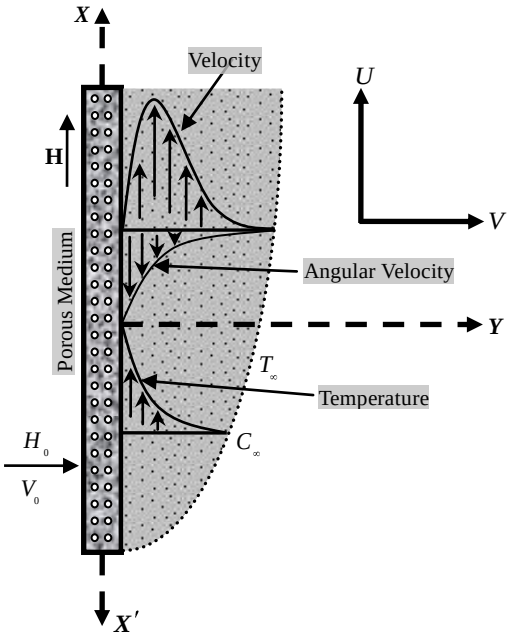

Fig 1. Physical Configuration and Coordinate System

In addition, the magnetic Reynolds number of the flow is taken to be large enough so that the induced magnetic field is of the form $\mathbf{H} = H_x, H_y, 0$ is applicable. The divergence equation of Maxwell's equation $\nabla.\mathbf{H} = 0$ for the magnetic field gives H_y = constant = H_0 (say). It is considered that the microrotation vector is of the form $\mathbf{G} = 0, 0, \overline{\Gamma}$ and the plate is of infinite extent with the fluid motion is unsteady, hence all the flow variables will depend only upon *y* and time.

Within the framework of the above stated assumptions and using the dimensionless quantities,

$$v = -V_0 \ , \ Y = \frac{yV_0}{\upsilon} \ , \ U = \frac{u}{V_0} \ , \ t = \frac{\tau V_0^2}{\upsilon} \ , \ \Gamma = \frac{\overline{\Gamma}\upsilon}{V_0^2} \ ,$$

$$H = \sqrt{\frac{\mu_e}{\rho}}\frac{H_x}{V_0} \ , \ T = \frac{\kappa V_0 \ \overline{T} - T_\infty}{Q\upsilon} \ , \ C = \frac{D_m V_0 \ \overline{C} - C_\infty}{m\upsilon}$$

with parameters, $G_r = \dfrac{g\beta Q\upsilon^2}{\kappa V_0^4}$, $G_m = \dfrac{g\beta^* m\upsilon^2}{D_m V_0^4}$,

$$\Delta = \frac{\chi}{\upsilon\rho} \ , \ M = \frac{H_0}{V_0}\sqrt{\frac{\mu_e}{\rho}} \ , \ P_m = \upsilon\sigma\mu_e \ , \ D_a = \frac{\upsilon^2}{V_0^2 K} \ ,$$

$$E_c = \frac{\kappa V_0^3}{Q\upsilon c_p} \ , \ \lambda = \frac{\upsilon\chi}{\rho j V_0^2} \ , \ P_r = \frac{\upsilon\rho c_p}{\kappa} \ , \ S_c = \frac{\upsilon}{D_m} \ ,$$

$S_o = \dfrac{Q D_m^2 \kappa_T}{m\kappa\upsilon c_s c_p}$, $\Lambda = \dfrac{\gamma}{\upsilon j \rho}$ as well as $\alpha = \dfrac{Q\upsilon^2}{\kappa V_0^2}$, the equations relevant to the unsteady problem are governed by the following non-dimensional system of coupled non-linear partial differential equations under the boundary-layer approximations,

$$\frac{\partial U}{\partial t} - \frac{\partial U}{\partial Y} = G_r T + G_m C + (1+\Delta)\frac{\partial^2 U}{\partial Y^2} + \Delta\frac{\partial \Gamma}{\partial Y} - D_a U + M\frac{\partial H}{\partial Y}$$

$$\frac{\partial \Gamma}{\partial t} - \frac{\partial \Gamma}{\partial Y} = \Lambda\frac{\partial^2 \Gamma}{\partial Y^2} - \lambda\left(2\Gamma + \frac{\partial U}{\partial Y}\right)$$

$$\frac{\partial H}{\partial t} - \frac{\partial H}{\partial Y} = M\frac{\partial U}{\partial Y} + \frac{1}{P_m}\frac{\partial^2 H}{\partial Y^2}$$

$$\frac{\partial T}{\partial t} - \frac{\partial T}{\partial Y} = \frac{1}{P_r}\frac{\partial^2 T}{\partial Y^2} + (1+\Delta)E_c\left(\frac{\partial U}{\partial Y}\right)^2 + \frac{E_c}{P_m}\left(\frac{\partial H}{\partial Y}\right)^2 - \frac{\alpha}{P_r}T$$

$$\frac{\partial C}{\partial t} - \frac{\partial C}{\partial Y} = \frac{1}{S_c}\frac{\partial^2 C}{\partial Y^2} + S_o\frac{\partial^2 T}{\partial Y^2}$$

also the appropriate initial and boundary conditions are given below when the plate is subjected to constant heat and mass fluxes,

$t \le 0, \ U = 0, \ \Gamma = 0, \ H = 0, \ T = 0, \ C = 0$ everywhere

$t > 0, \ U = 0, \ \Gamma = -s\dfrac{\partial U}{\partial Y}$, $H = 1, \dfrac{\partial T}{\partial Y} = \dfrac{\partial C}{\partial Y} = -1$ at $Y = 0$

$U = 0, \ \Gamma = 0, \ H = 0, \ T = 0, \ C = 0$ as $Y \to \infty$

3. NUMERICAL SOLUTIONS

To solve the above non-dimensional system by the unconditionally stable implicit finite difference method, it is required a set of finite difference equations. In this case, the region within the boundary layer is divided by some perpendicular lines of *Y* axis, where *Y*-axis is normal to the plate as shown in Fig. 2.

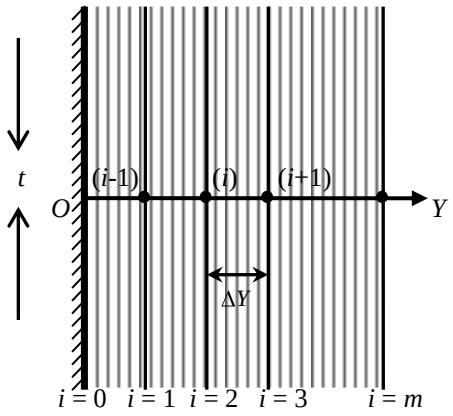

Fig 2. Finite difference grid system

It is assumed that the maximum length of boundary layer

is $Y_{\max} = 20$ as corresponds to $Y \to \infty$ i.e. Y varies from 0 to 20 and the number of grid spacing in Y directions is $m = 100$, hence the constant mesh size along Y axis becomes $\Delta Y = 0.20 \quad 0 \le Y \le 20$ with a smaller time-step $\Delta t = 0.01$.

Using the implicit finite difference approximations, we have the following appropriate set of finite difference equations,

$$\frac{U_i^{n+1} - U_i^n}{\Delta t} - \frac{U_{i+1}^n - U_i^n}{\Delta Y} = G_r T_i^n + G_m C_i^n + M \frac{H_{i+1}^n - H_i^n}{\Delta Y}$$

$$-D_a U_i^n + \left(1 + \Delta\right) \frac{U_{i+1}^n - 2U_i^n + U_{i-1}^n}{\Delta Y^2} + \Delta \frac{\Gamma_{i+1}^n - \Gamma_i^n}{\Delta Y}$$

$$\frac{\Gamma_i^{n+1} - \Gamma_i^n}{\Delta t} - \frac{\Gamma_{i+1}^n - \Gamma_i^n}{\Delta Y} = \Lambda \frac{\Gamma_{i+1}^n - 2\Gamma_i^n + \Gamma_{i-1}^n}{\Delta Y^2} - \lambda \left(2\Gamma_i^n + \frac{U_{i+1}^n - U_i^n}{\Delta Y} \right)$$

$$\frac{H_i^{n+1} - H_i^n}{\Delta t} - \frac{H_{i+1}^n - H_i^n}{\Delta Y} = \frac{1}{P_m} \frac{H_{i+1}^n - 2H_i^n + H_{i-1}^n}{\Delta Y^2} + M \frac{U_{i+1}^n - U_i^n}{\Delta Y}$$

$$\frac{T_i^{n+1} - T_i^n}{\Delta t} - \frac{T_{i+1}^n - T_i^n}{\Delta Y} = \frac{1}{P_r} \frac{T_{i+1}^n - 2T_i^n + T_{i-1}^n}{\Delta Y^2} + \frac{E_c}{P_m} \left(\frac{H_{i+1}^n - H_i^n}{\Delta Y} \right)^2$$

$$+ \left(1 + \Delta\right) E_c \left(\frac{U_{i+1}^n - U_i^n}{\Delta Y} \right)^2 - \frac{\alpha}{P_r} T_i^n$$

$$\frac{C_i^{n+1} - C_i^n}{\Delta t} - \frac{C_{i+1}^n - C_i^n}{\Delta Y} = \frac{1}{S_c} \frac{C_{i+1}^n - 2C_i^n + C_{i-1}^n}{\Delta Y^2} + S_o \frac{T_{i+1}^n - 2T_i^n + T_{i-1}^n}{\Delta Y^2}$$

with the finite difference initial and boundary conditions,

$$U_i^0 = 0, \quad G_i^0 = 0, \quad H_i^0 = 0, \quad T_i^0 = 0, \quad C_i^0 = 0$$

$$U_0^n = 0, \quad G_0^n = -s\left(\frac{U_1^n - U_0^n}{\Delta Y}\right), \quad H_0^n = 1,$$

$$T_1^n = T_0^n - \Delta Y, \quad C_1^n = C_0^n - \Delta Y$$

$$U_L^n = 0, \; G_L^n = 0, \; H_L^n = 0, \; T_L^n = 0, \; C_L^n = 0 \quad \text{where } L \to \infty$$

Here the subscript i designates the grid points with Y coordinate and the superscript n represents a value of time, $t = n\Delta t$ where $n = 0, 1, 2, 3, 4, \ldots\ldots\ldots\ldots$. The velocity, angular velocity, induced magnetic field, temperature and concentration at all interior nodal points may be computed by successive applications of the above finite difference equations.

4. RESULTS AND DISCUSSION

To investigate the practical situation of the problem, we have obtained the numerical values of the dimensionless velocity, angular velocity, induced magnetic field, temperature and concentration within the boundary layer for the turbulent boundary layer flow i.e. the value of microrotational constant(s) is chosen 1.0. Because of the great importance of cooling problem in nuclear engineering in connection with the cooling of reactors, the value of the Grashof number and modified Grashof number for heat transfer is taken positive. Since the most important fluids are atmospheric air, salt water and water so the results are limited to $P_r = 0.71$ (Prandtl number for air at 20° C), $P_r = 1.0$ (Prandtl number for salt water at 20° C) and $P_r = 7.0$ (Prandtl number for water at 20° C). In this study, the values of other parameters are chosen arbitrarily.

In order to get the steady state solutions of the problem, the computations have been carried out upto $t = 10$. We observed that the values of this computation, however, show little changes after $t = 4$. Thus the solution at $t = 10$ are essentially steady-state solutions. Hence the velocity, angular velocity, induced magnetic field, temperature and concentration profiles are drawn at $t = 1.0,\ 2.0$ and 10.0 .

The velocity, angular velocity, induced magnetic field, temperature and concentration distributions verses Y are illustrated in Figs. 3-18. The effect of the magnetic force number on the velocity field is presented in Fig. 3. It is observed that U decreases near the plate in case of strong M but far away from the plate the increase of M leads to an increase in velocity. The effect of Darcy number on the velocity field is plotted in Fig. 4. From this figure we see that the velocity decreases with the increase of D_a . Fig. 5 shows that the velocity increases in case of strong G_r . We see in Fig. 6, the rise of S_o leads to an increase in velocity. A decreasing affect on velocity field for P_r is observed from Fig. 7.

The effect of the spin gradient viscosity number on the angular velocity field is displayed in Fig. 8 and we see that the angular velocity decreases with the rise of Λ. Fig. 9 shows, the angular velocity is increasingly affected by λ. The effect of Schmidt number on the angular velocity field is presented in Fig. 10 and an increasing effect on the angular velocity profiles are observed from the figure in case of strong S_c .

Fig. 11 represents the effect of S_o on the induced magnetic field and it is observed from the figure the induced magnetic field decreases with the increase of S_o . A decreasing affect on induced magnetic field for P_m is observed from Fig. 12. In Fig. 13, we see that the induced magnetic field increases in case of strong Prandtl number. An increasing effect on the fluid temperature for the Schmidt number is highlighted in Fig. 14.

The temperature distributions are shown in Figs. 15-16 for different values of S_o and P_r . It is observed from the Fig. 15, the temperature weakly increases for the rise of S_o . The Fig. 16 shows that the temperature decreases with the rise of P_r .

For the different values of P_r and S_c , the species concentration curves are displayed in Figs. 17-18. We see in Fig. 17, the species concentration decreases with the rise of P_r . A decreasing effect on the concentration profiles is observed from the Fig. 18.

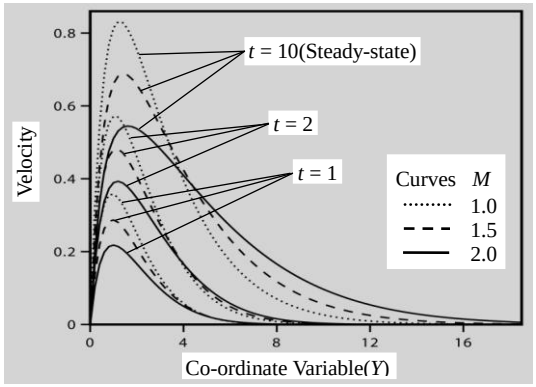

Fig. 3. Velocity Profiles for $G_m = 1$, $G_r = 2$, $\Lambda = 1$, $\lambda = 1$, $S_o = 1$, $D_a = 1$, $P_r = .71$, $P_m = 1$, $\Delta = 1$, $\alpha = 1$, $S_c = .6$ & $E_c = .01$.

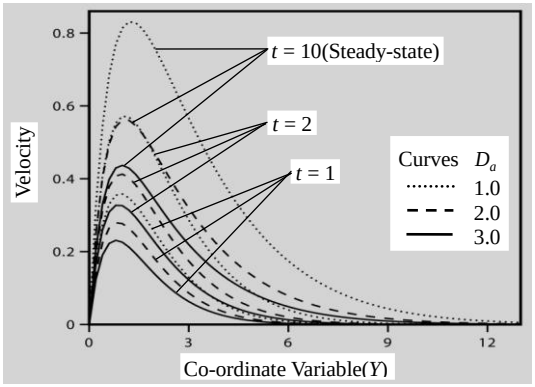

Fig. 4. Velocity Profiles for $G_m = 1$, $G_r = 2$, $\Lambda = 1$, $\lambda = 1$, $S_o = 1$, $M = 1$, $P_r = .71$, $P_m = 1$, $\Delta = 1$, $\alpha = 1$, $S_c = .6$ & $E_c = .01$.

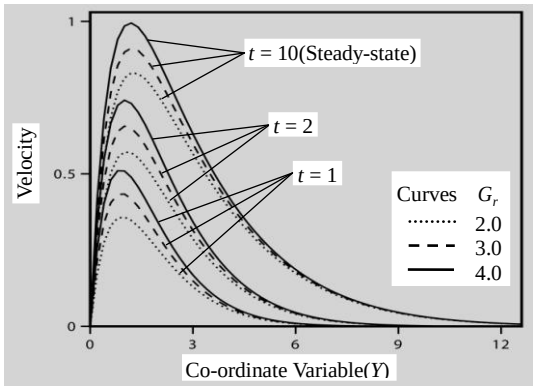

Fig. 5. Velocity Profiles for $G_m = 1$, $M = 1$, $\Lambda = 1$, $\lambda = 1$, $S_o = 1$, $D_a = 1$, $P_r = .71$, $P_m = 1$, $\Delta = 1$, $\alpha = 1$, $S_c = .6$ & $E_c = .01$.

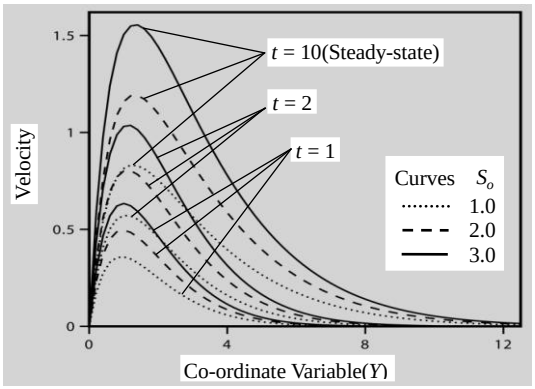

Fig. 6. Velocity Profiles for $G_m = 1$, $G_r = 2$, $\Lambda = 1$, $\lambda = 1$, $M = 1$, $D_a = 1$, $P_r = .71$, $P_m = 1$, $\Delta = 1$, $\alpha = 1$, $S_c = .6$ & $E_c = .01$.

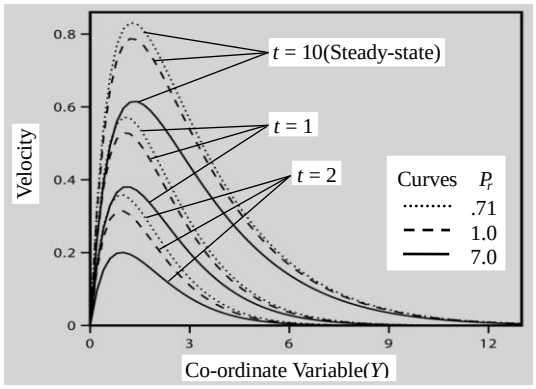

Fig. 7. Velocity Profiles for $G_m = 1$, $G_r = 2$, $\Lambda = 1$, $\lambda = 1$, $M = 1$, $D_a = 1$, $S_o = 1$, $P_m = 1$, $\Delta = 1$, $\alpha = 1$, $S_c = .6$ & $E_c = .01$.

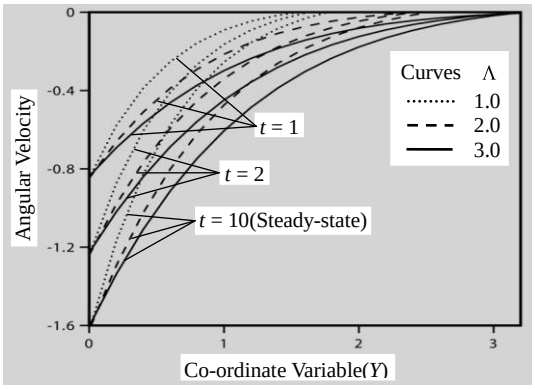

Fig. 8. Angular Velocity for $G_m = 1$, $G_r = 2$, $M = 1$, $\lambda = 1$, $S_o = 1$, $D_a = 1$, $P_r = .71$, $P_m = 1$, $\Delta = 1$, $\alpha = 1$, $S_c = .6$ & $E_c = .01$.

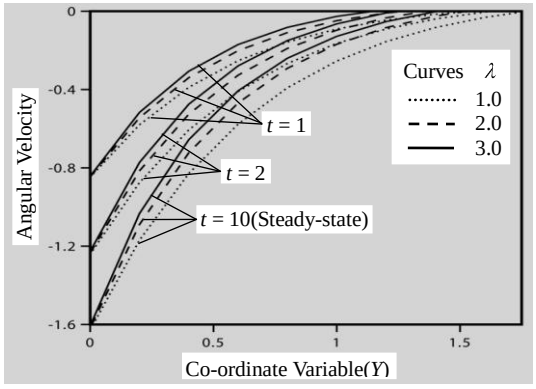

Fig. 9. Angular Velocity for $G_m = 1$, $G_r = 2$, $M = 1$, $\Lambda = 1$, $S_o = 1$, $D_a = 1$, $P_r = .71$, $P_m = 1$, $\Delta = 1$, $\alpha = 1$, $S_c = .6$ & $E_c = .01$.

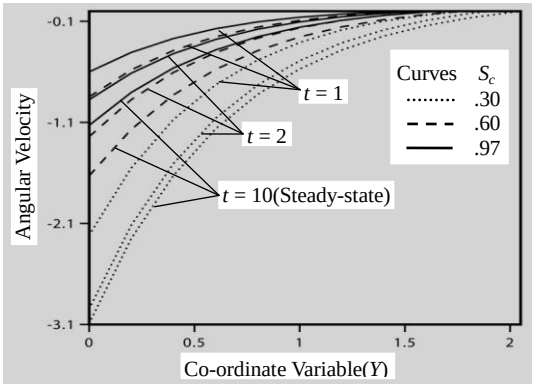

Fig. 10. Angular Velocity for $G_m = 1$, $G_r = 2$, $M = 1$, $\lambda = 1$, $S_o = 1$, $D_a = 1$, $P_r = .71$, $P_m = 1$, $\Delta = 1$, $\alpha = 1$, $\Lambda = 1$, & $E_c = .01$.

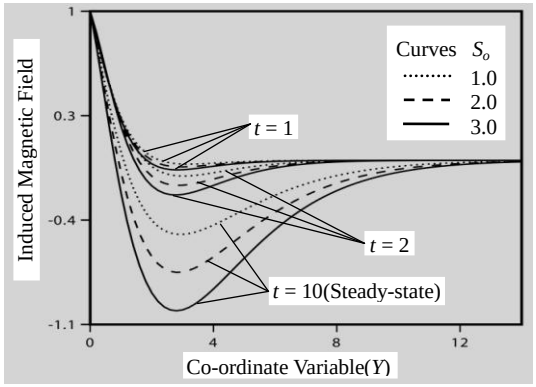

Fig. 11. Induced Magnetic Field for $G_m = 1,\ G_r = 2,\ \Lambda = 1,$ $M = 1,\ D_a = 1,\ P_r = .71,\ P_m = 1,\ \Delta = 1,\ \alpha = 1,\ S_c = .6$ & $E_c = .01$.

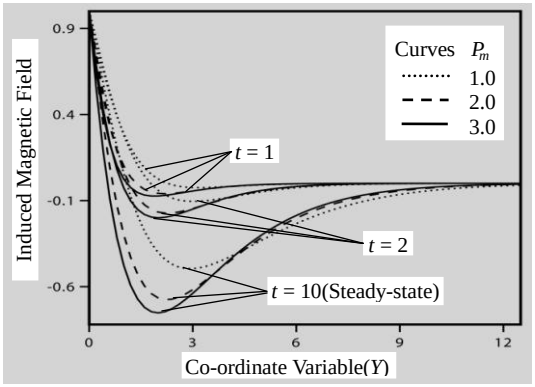

Fig. 12. Induced Magnetic Field for $G_m = 1,\ G_r = 2,\ \Lambda = 1,$ $M = 1,\ D_a = 1,\ P_r = .71,\ S_o = 1,\ \Delta = 1,\ \alpha = 1,\ S_c = .6$ & $E_c = .01$.

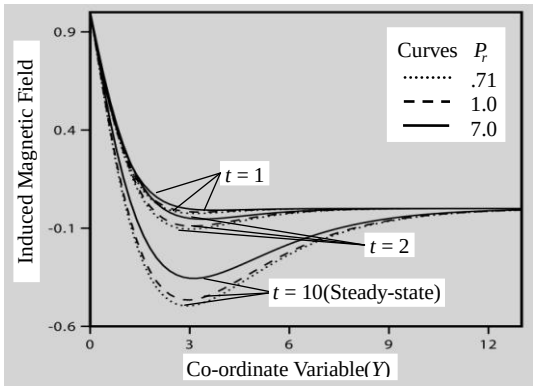

Fig. 13. Induced Magnetic Field for $G_m = 1,\ G_r = 2,\ \Lambda = 1,$ $M = 1,\ D_a = 1,\ S_o = 1,\ P_m = 1,\ \Delta = 1,\ \alpha = 1,\ S_c = .6$ & $E_c = .01$.

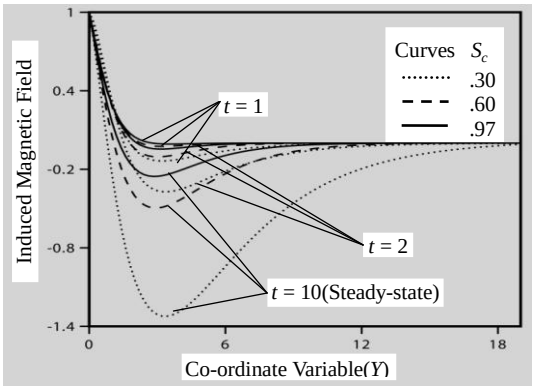

Fig. 14. Induced Magnetic Field for $G_m = 1,\ G_r = 2,\ \Lambda = 1,$ $M = 1,\ D_a = 1,\ P_r = .71,\ P_m = 1,\ \Delta = 1,\ \alpha = 1,\ S_o = 1,$ & $E_c = .01$.

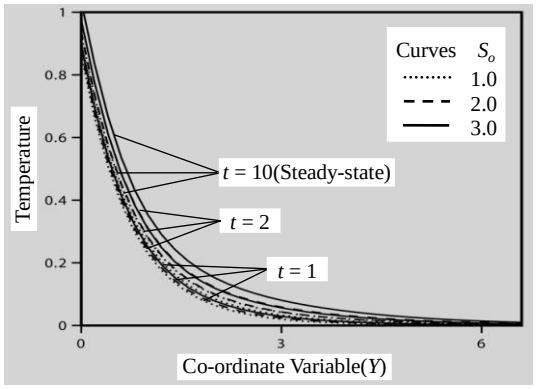

Fig. 15. Temperature for $G_m = 1,\ G_r = 2,\ \Lambda = 1,\ \lambda = 1,\ M = 1,$ $D_a = 1,\ P_r = .71,\ P_m = 1,\ \Delta = 1,\ \alpha = 1,\ S_c = .6$ & $E_c = .01$.

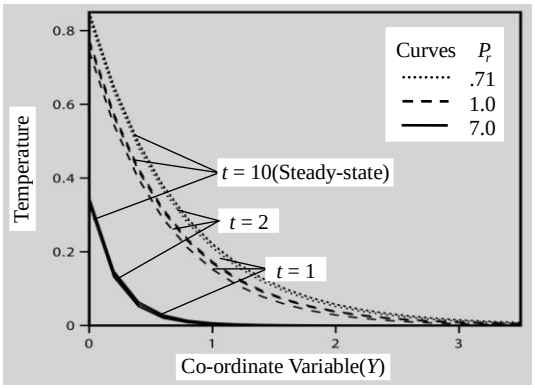

Fig. 16. Temperature for $G_m = 1,\ G_r = 2,\ \Lambda = 1,\ \lambda = 1,\ M = 1,$ $D_a = 1,\ S_o = 1,\ P_m = 1,\ \Delta = 1,\ \alpha = 1,\ S_c = .6$ & $E_c = .01$.

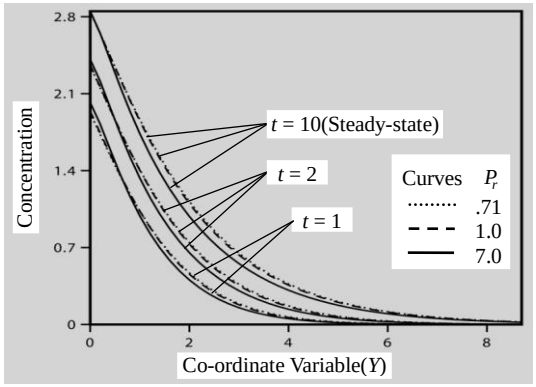

Fig. 17. Concentration for $G_m = 1,\ G_r = 2,\ \Lambda = 1,\ \lambda = 1,$ $M = 1,\ D_a = 1,\ S_o = 1,\ P_m = 1,\ \Delta = 1,\ \alpha = 1,\ S_c = .6$ & $E_c = .01$.

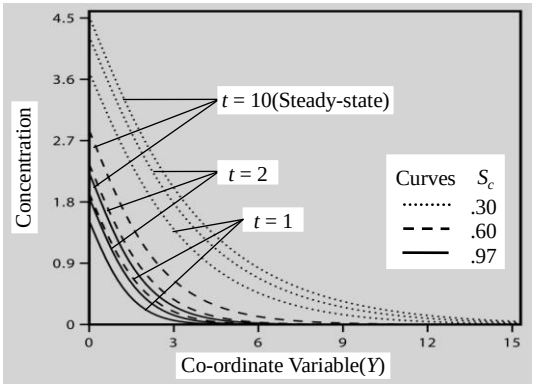

Fig. 18. Concentration for $G_m = 1,\ G_r = 2,\ \Lambda = 1,\ \lambda = 1,$ $M = 1,\ D_a = 1,\ S_o = 1,\ P_m = 1,\ \Delta = 1,\ \alpha = 1,\ P_r = .71$ & $E_c = .01$.

Finally, a qualitative comparison of the recent result at steady-state with the previous result of the MHD free convective heat generating unsteady micropolar fluid flow through a porous medium given by Haque et al.[7] is presented in Table 1. In case of cooling of the plate, the present problem with the absence of the induced magnetic field reduces to the problem that investigated by Haque et al.[7]. The accuracy of the recent results may be described as good in case of all the flow variables.

Table 1: Qualitative comparison of the present result with previous result of approximate solutions

Increased Parameter	Previous Results due to Haque et al.[7]				Present Results of Numerical Solution			
	U	Γ	*T*	*C*	*U*	Γ	*T*	*C*
M	Dec.	Inc.	No Ef.	No Ef.	Dec.	No Ef.	No Ef.	No Ef.
G_r	Inc.	Dec.	No Ef.	No Ef.	Inc.	No Ef.	No Ef.	No Ef.
S_o	Inc.	Dec.	No Ef.	Inc.	Inc.	No Ef.	Inc.	No Ef.
P_r	Dec.	Inc.	Dec.	Dec.	Dec.	No Ef.	Dec.	Dec.
S_c	Dec.	Inc.	No Ef.	Dec.	No Ef.	Inc.	No Ef.	Dec.

5. CONCLUSIONS

In this work thermal diffusion effects on the free convective heat and mass transfer MHD unsteady flow of a micropolar fluid through a porous medium with induced magnetic field is investigated. The resulting governing equations are solved by implicit finite difference method. The obtained results are graphically presented for the variations of associated parameters. Some of the important findings of this observation are given below,

i. For the cooling plate, the micropolar fluid velocity increases with the increase of Grashof number.
ii. The micropolar fluid velocity is more for air than water.
iii. The angular velocity is greater for heavier particle than lighter particle.
iv. The induced magnetic field is more for water than air.
vi. The fluid temperature is higher for air than water.
vii. The species concentration is greater for lighter particle than heavier particle.

It is hoped that the findings of the present work may be useful for the study of astrophysics and geophysics.

6. REFERENCES

1. Chaudhary, R.C. and Sharma, B.K., 2006, "Combined heat and mass transfer by laminar mixed convection flow from a vertical surface with induced magnetic field", J. of Applied Physics, 99:034901.
2. Alam, M.M., Islam, M.R. and Rahman, F., 2008, "Steady heat and mass transfer by mixed convection flow from a vertical porous plate with induced magnetic field, constant heat and mass fluxes", Tham. Int. J. of Sci. and Tech., 13(4):1.
3. Haque, M.M. and Alam, M.M., 2009, "Transient heat and mass transfer by mixed convection flow from a vertical porous plate with induced magnetic field, constant heat and mass fluxes", AMSE Journal, 78(4):54.
4. Eringen, A.C., 1966, "Theory of micropolar fluids", Journal of Mathematics and Mechanics, 16:1.
5. Jena, S.K. and Mathur, M.N., 1981, "Similarity solution for laminar free convection flow of thermomicropolar fluid past a non-isothermal vertical flat plate", Int. J. of Eng. Sci., 19:1431.
6. El-Amin, M.F., 2001, "Magnetohydrodynamic free convection and mass transfer flow in micropolar fluid with constant suction", J. of Magnetism and Magnetic Materials, 234:567.
7. Haque, M.M., Alam, M.M., Ferdows, M. and Postelnicu, A., 2011, "MHD free convective heat generating unsteady micropolar fluid flow through a porous medium with constant heat and mass fluxes", European Journal of Scientific Research, 53(3):491.

7. NOMENCLATURE

Symbol	Meaning	Unit
x, y	Cartesian coordinates	
u, v	Velocity components	(ms^{-1})
υ	Kinematic viscosity	(m^2s^{-1})
ρ	Density of fluid	(kgm^{-3})
μ_e	Magnetic permeability	
t	Dimensionless time	
X, Y	Dimensionless cartesian coordinates	
U, V	Dimensionless velocity components	
V_0	Constant suction velocity	
H_x, H_y	Induced magnetic field components	
H	Dimensionless induced magnetic field component	
$\overline{\Gamma}$	Micro-rotational component	
C	Dimensionless concentration	
T	Dimensionless temperature	
κ	Thermal conductivity	
D_m	Coefficient of mass diffusivity	
Q	Constant heat flux per unit area	
m	Constant mass flux per unit area	
g	Local acceleration due to gravity	
β	Thermal expansion coefficient	
β^*	Concentration expansion coefficient	
G_r	Grashof number	
G_m	Modified Grashof number	
Δ	Micro-rotational number	
M	Magnetic force number	
P_m	Magnetic diffusivity number	
D_a	Darcy number	
P_r	Prandtl number	
E_c	Eckert number	
λ	Vortex viscosity	
S_c	Schmidt number	
S_o	Soret number	
Λ	Spin gradient viscosity number	
α	Heat source number	
s	Microrotational constant	

8. MAILING ADDRESS

Md. Mohidul Haque
Mathematics Discipline,
Khulna University,
Khulna-9208, Bangladesh
E-mail: alam_mahmud2000@yahoo.com